RESEARCH ARTICLE

Projected changes in the season of hot days in the Middle East and North Africa

Rubén Varela[1] ![ORCID] | Laura Rodríguez-Díaz[1] | David Barriopedro[2,3] |
Maite de Castro[1] | Xurxo Costoya[4] | Ricardo García-Herrera[2,3] |
Moncho Gómez-Gesteira[1]

[1]Environmental Physics Laboratory (EphysLab), CIM-UVIGO, Universidade de Vigo, Ourense, Spain

[2]Dpto. Fisica de la Tierra II, Facultad de Ciencias Físicas, Universidad Complutense de Madrid, Madrid, Spain

[3]IGEO, Instituto de Geociencias (Consejo Superior de Investigaciones Científicas (CSIC), Universidad Complutense de Madrid (UCM)), Madrid, Spain

[4]Group of Nonlinear Physics, Faculty of Physics, CRETUS, University of Santiago de Compostela, Santiago de Compostela, Spain

Correspondence
R. Varela, Environmental Physics Laboratory (EphysLab), CIM-UVIGO, Universidade de Vigo, Edificio Campus da Auga, 32004 Ourense, Spain.
Email: ruvarela@uvigo.es

Funding information
European Regional Development Fund, Grant/Award Numbers: EU. INTERREG-POCTEP 2014-2020, 0034-RISC_ML_6_E; Xunta de Galicia, Grant/Award Number: ED431C 2017/64-GRC

Abstract

The present study analyses changes in the timing and duration of the hot days season over the Middle East and North Africa region from 1970 to 2099 using model simulations of 11 regional models from the Coordinated Regional Climate Downscaling Experiment under the RCP8.5 scenario. In general, a non-symmetrical lengthening of the hot days season is projected, with a tendency to extend more into spring than into autumn. By the end of the century and the RCP8.5 scenario, Western Africa and the Persian Gulf display a hot days season starting 60 days earlier than in the historical period (1970–1999) (May vs. July, respectively). Southernmost latitudes are the most affected by a later retreat of the hot days season, of up to 60 days with respect to the historical period (October vs. August). The length of the extreme season is projected to increase between 100 and 120 days for the southernmost latitudes and the Persian Gulf resulting in nearly four more months with hot days conditions.

KEYWORDS

climate change, CORDEX, extreme temperatures, future projections, hot days season, Iberian Peninsula, MENA, Turkey

1 | INTRODUCTION

Changes in the annual cycle of temperature are one of the reported impacts of climate change and they have been the focus of different studies (Christidis *et al*., 2007; Stine *et al*., 2009; Peña-Ortiz *et al*., 2015; Cassou and Cattiaux, 2016). Stine *et al*. (2009) described the changes in the phase of the annual cycle of surface temperature between 1954 and 2007. They reported a shift of 1.7 days·decade⁻¹ towards earlier seasons over extratropical land with some regional differences. Peña-Ortiz *et al*. (2015) assessed the multidecadal variability of the summer length in Europe for the period 1950–2012. They obtained an enlargement

of the summer season particularly prominent since 1979, and related it to mean temperature trends during June and September, which affected the summer onset and end dates.

The observed rise of temperatures and the associated summer lengthening are accompanied by an increase of extreme events as heat waves (e.g., Murray and Ebi, 2012). Perkins-Kirkpatrick and Lewis (2020) reported a significant increasing trend in heat wave frequency, duration and cumulative heat since 1950, albeit with regional differences. In particular, some of the largest trends stood out in the Middle East and North Africa (MENA) region (Ntoumos et al., 2020). This is also one of the regions experiencing the most dramatic changes in future projections, even for a 1.5°C global warming target with respect to pre-industrial conditions (e.g., Perkins-Kirkpatrick and Gibson, 2017; Russo et al., 2019a). Argueso et al. (2016) found that the projected changes to longer, more frequent and more intense heat waves by the end of the 21st century are largely controlled by mean temperature changes. Hotter and longer summers are also expected to affect the seasonality of heat waves, which would occur earlier and closer to the spring, and latter into the fall, in agreement with unusual recent heat wave events (Sánchez-Benítez et al., 2018) and the observed lengthening of the summer season (Peña-Ortiz et al., 2015).

These seasonal shifts (summer lengthening and changes in the seasonality of extreme events) imply changes in risks due to increased exposure to hazards associated with high temperatures. Changes in the warm season could imply a heat-related mortality increase and other heat wave risks, particularly in low-development countries (Russo et al., 2019a). For example, Sheridan and Lin (2014) reported an increment of mortality excess in New York due to changes in the onset of heat wave season. Muthers et al. (2010) concluded that the mortality impact of early heat waves in Vienna was higher than the impact of heat waves of the same magnitude in late summer, in agreement with the so-called harvesting effect (e.g., García-Herrera et al., 2010; deCastro et al., 2011). These seasonality changes would also imply alterations in the exposure to vectors of infectious diseases, by altering the timing when they can develop (Smith et al., 2014; Watts et al., 2015). Outdoor activity should be reduced to avoid exposure to heat waves (Watts et al., 2019, 2020), therefore affecting key activities such as agriculture, particularly for the main global producers. Agriculture production itself could also be affected, as during recent devastating events (Barriopedro et al., 2011; Kornhuber et al., 2020), being aggravated in regions with reported synergies between heat wave and droughts (e.g., Miralles et al., 2019; Russo et al., 2019b). Moreover, a shift to an earlier occurrence of heat waves can challenge the energy

systems due to the increase in energy demand for air conditioning (Hameed et al., 2019; Lange, 2019).

Therefore, analysing changes in the seasonality of temperature extremes is of the outmost importance, especially in the most vulnerable countries, such as those located in the MENA region. This region has been experiencing a continuous rise in temperatures since the 20th century that will persist during the 21st century (Evans, 2009; Niang et al., 2014; Giugni et al., 2015; Pal and Eltahir, 2016; Ozturk et al., 2018; Varela et al., 2020). This is accompanied by a robust increase in extreme temperatures and heat waves (Lelieveld et al., 2016; Russo et al., 2016; Dosio, 2017; Bucchignani et al., 2018; Varela et al., 2020). Varela et al. (2020) reported a general increase of extreme temperature conditions over the MENA region for the 21st century, with more than 80% of the cities experiencing heat wave conditions during at least 50% of the warm season days. Almazroui (2019) and Driouech et al. (2020) found a general rise in the number of hot days with increasing rates up to 10 days· decade^{-1}. However, to the best of our knowledge, future changes in the timing of current extreme conditions over the MENA region have not been reported in the literature. They would have pronounced impacts in several aspects. Regarding the socioeconomic consequences, the MENA region is characterized by important regional differences (Ncube et al., 2014). This fact, along with an overall low development, pose difficulties to conduct adaptation and mitigation policies and to deploy early warning systems (Göll, 2017; Borghesi and Ticci, 2019; Watts et al., 2020). Taking into account the current conditions and the fraction of people working in agriculture, industry and services, the areas of the MENA region with the largest heat-related lost in potential work hours are those situated in northwestern Africa and in the Persian Gulf (Watts et al., 2019, 2020). When climate change projections (2071–2099) are combined with estimated population heat exposure to moderate intensity jobs, the most affected areas are those situated in the southernmost latitudes of the MENA region, with around 10% work hours lost (Kjellstrom et al., 2018). These results delve into the special difficulties of the most vulnerable populations, causing other derived problems such as famine and climate-induced migrations (Grant et al., 2014; Wodon et al., 2014; Waha et al., 2017). Another important impact is the increase in heat-related mortality (Gasparrini et al., 2017; Mora et al., 2017; Ahmadalipour and Moradkhani, 2018). Ahmadalipour et al. (2019) found that the mortality risk from heat stress is expected to hit the poorest nations the hardest, increasing by a factor of 8–20 in the last decades of the 21st century with respect to the last decades of the 20th century for the MENA region. The particular characteristics of the MENA region [e.g., aridity, projected population increase from 341 million to

845 million in 2100; (Waha *et al.*, 2017)], make this region prone to be one of the most seriously affected by changes in the seasonality of extreme temperatures in the future (Waha *et al.*, 2017).

The main of this paper is to analyse how the hot days season (HdS), defined as the period of the year experiencing present-day extreme temperature conditions, will evolve under a warming climate in the MENA region. To assess these changes, the Coordinated Regional Climate Downscaling Experiment (CORDEX)-MENA regional model experiments are used. The start, end and length of the HdS are analysed for the historical period (1970–1999), and climate change projections under the RCP8.5 scenario, focusing on the near (2020–2049) and far (2070–2099) futures. Moreover, different areas of the MENA region are considered to assess regional differences.

2 | DATA AND METHODS

Daily maximum near-surface air temperature data were retrieved from 11 Regional Climate Model–Global Climate Model (RCM–GCM) pairs simulations of the CORDEX (https://www.cordex.org/data-access/) for the Africa domain. They include historical simulations for the 1970–2005 period and future projections (2006–2099) from 11 RCM–GCM pairs (one realization per pair) under the RCP8.5 greenhouse gas emission scenario (Taylor *et al.*, 2012). The list of models is displayed in Table S1.

The CORDEX simulations cover the domain [0, 42.24°N] and [20°W, 60.28°E] with a 0.44° × 0.44° spatial resolution (Christensen *et al.*, 2014). However, the MENA region analysed here is limited to the areas of the domain that extend north of 24°N, where there is a well-defined seasonal cycle in temperature. As can be seen in Figure 1, this domain includes hot spot areas for climate change [e.g., the Mediterranean (Giorgi and Lionello, 2008; Cramer *et al.*, 2018] and critical human habitability (e.g., Arabian Gulf; Pal and Eltahir, 2016). Previous
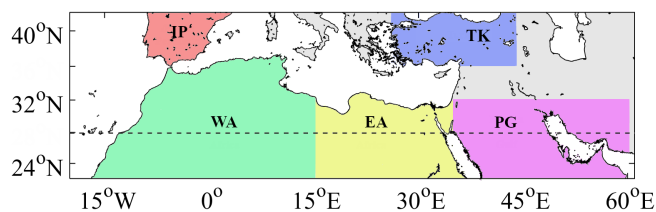

FIGURE 1 Map of the Middle East and North Africa (MENA region). Colour areas represent the sub-regions considered: IP (Iberian Peninsula), TK (Turkey), WA and EA (Western and Eastern Africa), PG (the Persian Gulf). The dashed line marks the 28°N meridian that divides the study area into the northern and southern regions [Colour figure can be viewed at wileyonlinelibrary.com]

studies (Dosio and Panitz, 2016; Ozturk *et al.*, 2018; Varela *et al.*, 2020) have widely used RCMs due to their capability to recreate extreme events at fine scales. In what concerns heat waves, the performance of CORDEX models over the historical period and the MENA region has been evaluated in previous studies, such as Russo *et al.* (2016) and Dosio (2017)).

To evaluate model performance, hourly 2 m temperature data were retrieved for the 1979–2005 period of ERA5, the fifth generation of the global reanalysis from the European Centre for Medium-Range Weather Forecasts (Hersbach *et al.*, 2020). For each day, the maximum temperature was selected and subsequently interpolated to the common 0.44° × 0.44° grid of the CORDEX simulations.

The season of hot days (HdS) was characterized by its start, end and length. HdS is defined as the period between the first day ($Start^{HdS}$) and the last day (End^{HdS}) that exceeded the local 95th percentile of the daily maximum temperature distribution for the historical period (all days of the year for the 1970–1999 period). $Start^{HdS}$ and End^{HdS} days are expressed in terms of their rank in the year (starting from January 1). The HdS length ($Length^{HdS}$) was computed as the difference between End^{HdS} and $Start^{HdS}$. HdS was calculated for each land grid point of the MENA region, year and model. Then, a multi-model mean was applied to the parameters defining HdS (start, end and length), in order to minimize biases associated with each single model (Pierce *et al.*, 2009; Jacob *et al.*, 2014). The choice of the HdS definition follows similar standardized approaches employed in the detection of extreme indices [e.g., TX90p of the Expert Team on Climate Change Detection and Indices (ETCCDI)], which does not require any duration criterion. This type of definition is quite common in works on climatic extremes (Easterling, 2002; Kunkel *et al.*, 2004; Peña-Ortiz *et al.*, 2015; Founda *et al.*, 2019). To impose a persistence criterion is not easy as it could be confused with the calculation of the earliest heat wave, which is not the objective of the present article. Note that several studies stress that heat waves represent a different type of extreme event, as compared to those represented by the extreme indices of the ETCCDI. The idea of considering the first day as the start of the HdS resides in the interest of developing early warning systems that can help to mitigate the extreme heat as the harvesting effect. Therefore, the HdS definition follows recent works such as that of Founda *et al.* (2019) and keeps the first and last days when the 95 percentile of the local daily maximum temperature is exceeded.

Spatial averages of the multi-model mean parameters were also computed for the whole MENA region and different sub-regions (Figure 1): Iberian Peninsula (IP), Turkey (TK), West and East Africa (WA and EA, respectively) and the Persian Gulf (PG). These sub-regions were selected following geographical and climatological criteria,

the latter mainly relying on the characteristics of HdS, as described in the results. Trends in the regional metrics of the HdS were calculated using the Spearman rank correlation coefficient.

To minimize the influence of internal variability, the annual local parameters (Start^{HdS}, End^{HdS} and Length^{HdS}) were also averaged for three different 30-year periods: historical (1970–1999), near future (2020–2049) and far future (2070–2099). Multi-model mean changes in these metrics were calculated as the difference between the future (near or far) and historical 30-year means. As stated above, the time of occurrence of hot days conditions with respect to the warmest peak of the year is of high importance in terms of the associated impacts (Watts *et al.*, 2015). To measure this, we compared the number of hot days in the near- and far-future HdS that fall outside and inside the historical HdS of the corresponding model. Their ratio quantifies the contribution to changes in the frequency of extremes from days that would not have yielded extreme conditions in the historical period.

A two-step procedure was applied to assess the robustness and significance of the changes in the HdS projected by the multi-model ensemble. In the first step, model agreement is tested and changes are considered robust when more than 90% of the RCM–GCM pairs project the same sign change as that of the multi-model mean. In the second step, significance is assessed with the Mann–Whitney *U* test to evaluate whether the historical and future samples of each model pair have equal medians. Changes are considered statistically significant when the null hypothesis is rejected in more than 66% of the models at 95% confidence level. Confidence arises when both conditions are met.

3 | RESULTS

3.1 | Evaluation of CORDEX simulations

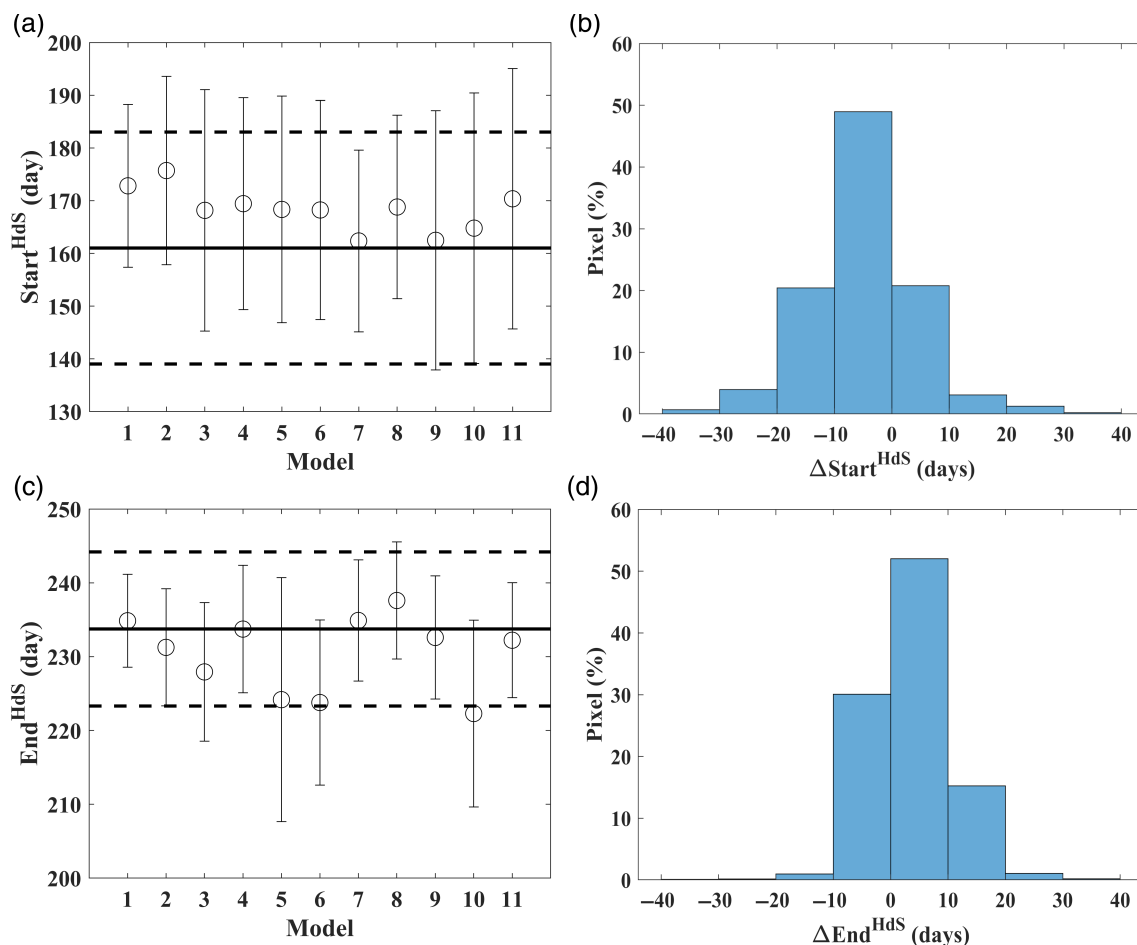We first assessed the skill of the CORDEX ensemble of historical simulations to reproduce the HdS of ERA5

FIGURE 2 Mean value (± 1 *SD*) of the season start (a) and end (c) for the common historical period for ERA5 (black solid line) and each CORDEX model (circles). The number of each model is referred to the Table S1. (b) and d) Histogram of the season start and end difference between the CORDEX multi-model mean and ERA5. In both cases, the difference means ERA5 minus CORDEX [Colour figure can be viewed at wileyonlinelibrary.com]

(1979–2005). a,c shows the climatological mean (± 1 *SD*) start and end of the HdS for the MENA region and each CORDEX RCM–GCM pair. All models show a small bias towards later onset of the HdS (higher Start^{HdS}), with small differences across the ensemble (i.e., similar individual model performance). The multi-model mean start date of the HdS does not deviate from ERA-5 by more than ~10 days, which means a relative error lower than 10%. There is a larger spread in the simulation of the end of the HdS, with a generalized tendency for an earlier retreat (i.e., lower End^{HdS}), but no systematic behaviour across the model ensemble. This result indicates that the ensemble is not dominated by the performance of the RCA4 model, which is employed in more than half of the RCM-GCM pairs (Table S1). The multi-model mean tends to compensate individual model biases in End^{HdS}, yielding a performance that is comparable to that of the onset (i.e., relative error lower than 10%). As a consequence, CORDEX models display a shorter HdS length than ERA5, likely reflecting an exaggerated seasonal cycle in mean temperature.

The frequency distribution of the multi-model mean local biases in the HdS timing across the MENA region is displayed in Figures 2b,d. In most of the region (~75% of the grid points) the differences between the multi-model mean and ERA5 do not exceed ~10 days. The spatial patterns of the start and end biases do not resemble each other (Figure S1), although EA tends to concentrate the largest biases in both parameters (albeit over different areas of this region).

Despite the expected differences between both databases, data from CORDEX reproduces satisfactorily the spatial patterns in the area under scope for the historical period. These results show the adequacy and robustness of the models. Therefore, in the following sections, we will use the full ensemble of CORDEX to address future projections of HdS in the MENA domain.

3.2 | Projected HdS changes

Figure 3 (left panel) displays the multi-model mean timing (start, end) and length of the HdS for the historical period over the MENA region. The middle and right panels show the start, end and length changes of the HdS for the near and far futures with respect to the historical period over the MENA region. For the historical period, WA and PG are the regions with a later start (around mid-July, or calendar day 180–200). In EA, this value decreases to 130–140, which corresponds approximately to mid-May (the earliest start within MENA). Figure S1a confirms that, in spite of the CORDEX biases, the multi-model mean captures the overall spatial pattern of ERA-5, including the earlier/later start of the HdS in EA/WP. In the case of the near future, the start of the season is projected to advance to earlier dates (i.e., negative changes in Start^{HdS}) by around 30 days for the southern areas of Northern Africa and PG, and 10–20 days for the rest of MENA. Larger changes are expected for the far future, with values ranging from 40 days over some areas of EA, to up to 60 days in WA and PG. Therefore, by the end of the century, the most affected areas are projected to start the HdS up to 2 months earlier than in the historical period (a shift from mid-July to mid-May over WA and PG).
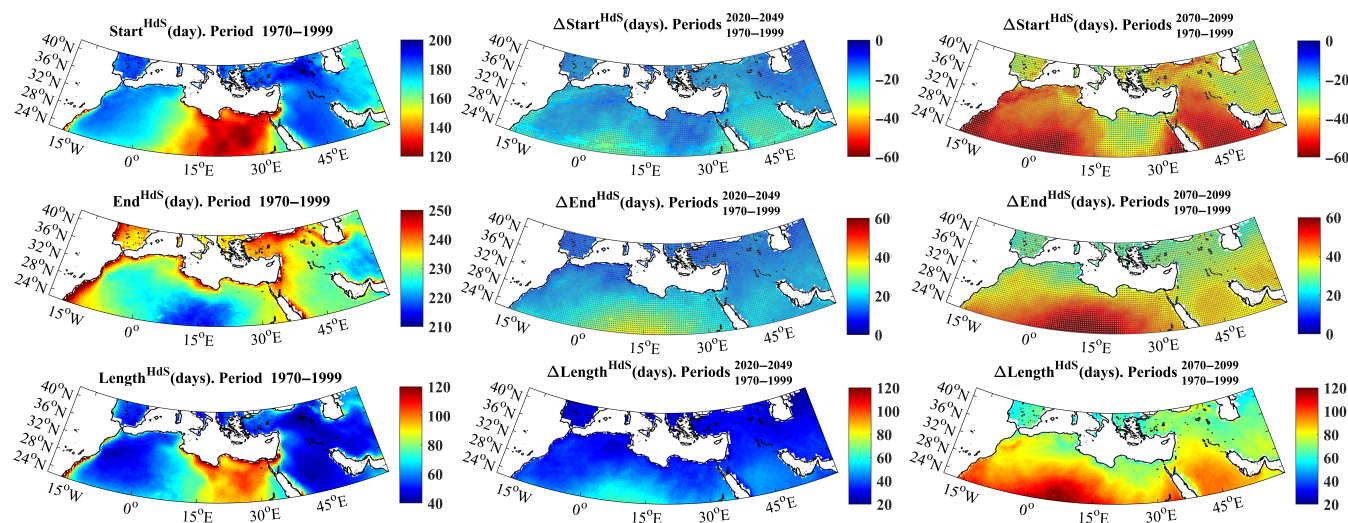

FIGURE 3 Multi-model mean characteristics (start, end and length) of the hot days season for the historical period (1970–1999; left column) and projected changes under the RCP8.5 scenario for the near (2020–2049; middle column) and far (2070–2099; right column) futures. Grey points mark those pixels that passed our confident assessment on the projected changes. See text for details [Colour figure can be viewed at wileyonlinelibrary.com]

Focusing on the End^{HdS} (middle row panels), it occurs by around mid-August (Days 220–230) for the historical period and most of the area, except for coastal regions and the northernmost sub-regions of MENA (IP, TK), where it occurs in early September (around Day 250). The earlier (later) retreat of the HdS in southern MENA (coastal regions, IP and TK) is in overall agreement with the ERA-5 pattern (Figure S1c). For the near future, all areas display a later retreat of the HdS (i.e., positive changes in End^{HdS}). The largest changes are obtained in southern central areas of Northern Africa, with values around 30 days. In the rest of MENA, the end of the HdS is delayed by 10–20 days, which represents smaller changes than those reported for Start^{HdS}. This geographical pattern is also observed for the far future, but with highest values that can reach 60 days in southern central MENA and around 30–40 days in the rest of the area. Thus, the southernmost latitudes are expected to experience the largest changes in the End^{HdS} (~2 months, from mid-August to mid-October) as compared to the historical period.

Regarding the Length^{HdS}, it ranges between 50 and 120 days across the MENA region for the historical period. EA shows the longest HdS and WA, PG, IP and TK the shortest one. The geographical pattern of changes in Length^{HdS} is very similar for both time horizons, with more pronounced changes for the far future. For the near future, the lengthening of the HdS ranges from 20 to 40 days in the northern latitudes of MENA, to up to 60 days in the southern latitudes. In a similar way, the far future shows a HdS that is 120 days longer than in the historical period over the southernmost latitudes, with lower changes in the rest of the area (typically below 80 days).

It is important to note that the lengthening of the HdS is not equally distributed towards earlier and later periods. Focusing on the far future (right column, Figure 3), changes in the season length come from a more noticeable shift towards earlier onsets than later retreats, especially for WA and PG. Only a small region in southern-central Northern Africa displays larger changes in End^{HdS} than in Start^{HdS} (top and middle panels, Figure 3).

This asymmetric lengthening of the HdS also becomes obvious at larger spatial scales. Figure 4 shows the start, end and length of the HdS averaged for the MENA region under the RCP8.5 scenario from 1970 to 2099. The slope for the start dates is larger (in absolute values) than that for the end dates (Figure 4a). In particular, the HdS onset (red) advances steadily from around Days 170 (end of June) to 120 (early May) by the end of the century, which is around 50 days earlier than in the historical period. In the same period, the End^{HdS} (blue) retreats about
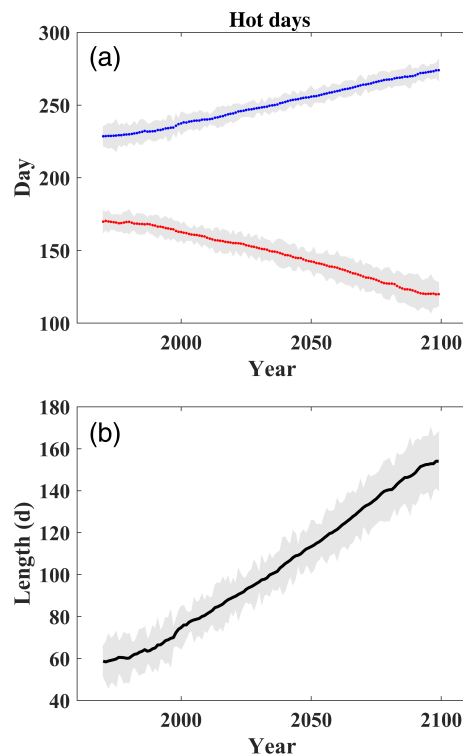

FIGURE 4 Multi-model mean (solid lines) annual evolution and inter-model spread (±1 *SD*, grey shading) of the hot days season for the MENA region during the historical period (1970–2005) and the RCP8.5 scenario (2006–2099): (a) start (red) and end (blue) of the hot days season. (b) Length of the hot days season [Colour figure can be viewed at wileyonlinelibrary.com]

40 days, from mid-August (Day 230) to late September–early October (Day 270). As a consequence, under RCP8.5, the HdS gets longer by more than 90 days through the 21st century (Figure 4b), increasing from less than 60 days in the historical period to nearly 160 days (5 months) by the end of the century.

Although the changes presented in Figure 4 summarize well the generalized behaviour of the MENA region, there are also quantitative regional differences (see Figure 3) that are herein addressed in more detail. Table 1 shows the 1970–2099 multi-model mean trend and *SD* of the HdS start, end and length for MENA and the different sub-regions of Figure 1 under the RCP8.5 scenario. WA and PG are the areas with the largest trends in Start^{HdS} (almost −0.5 day·year^{-1}) which are equivalent to an advance of about 2 months by the end of the century. This contrasts with the northernmost regions (IP and TK) and EA, where trends are smaller than −0.4 day·year^{-1} (i.e., ~45 days earlier onsets by 2100). These results suggest quantitative latitudinal differences in the changes of Start^{HdS}. Indeed, the southernmost areas of the MENA region (those equatorward of 28°N)

TABLE 1 Linear trend (days·year^{-1}) ($\pm$ 1 SD) of the multi-model mean start, end and length of the hot days season for each region of the MENA domain from 1970 to 2099 under the RCP8.5 scenario

REGION	START$_T$ (days·year^{-1})	END$_T$ (days·year^{-1})	LENGTH$_T$ (days·year^{-1})
Iberian Peninsula	−0.35 ± 0.06	0.28 ± 0.04	0.63 ± 0.09
Turkey	−0.39 ± 0.09	0.29 ± 0.05	0.69 ± 0.13
West Africa	−0.49 ± 0.09	0.42 ± 0.08	0.91 ± 0.16
East Africa	−0.37 ± 0.08	0.43 ± 0.11	0.80 ± 0.15
Persian Gulf	−0.46 ± 0.11	0.38 ± 0.04	0.83 ± 0.14
South 28°N	−0.48 ± 0.09	0.45 ± 0.08	0.93 ± 0.16
North 28°N	−0.39 ± 0.07	0.33 ± 0.06	0.73 ± 0.12
MENA	−0.43 ± 0.07	0.38 ± 0.06	0.80 ± 0.13

show the most dramatic changes in Start^{HdS} (−0.48 as compared to −0.39 day·year^{-1}, for regions poleward of 28°N; Table 1), which translate to differences of almost half a month by 2100. A similar latitudinal behaviour is observed for End^{HdS}, with delays that are about half a month longer in the southernmost latitudes than in the northern regions by the end of the century (Table 1). Therefore, IP and TK experience lower changes in End^{HdS} (smaller than 0.30 day·year^{-1}) than more equatorward regions (e.g., WA or EA, higher than 0.40 day·year^{-1}). Except for EA, the rest of the regions show higher trends (in absolute terms) for Start^{HdS} than for the End^{HdS}, confirming the overall asymmetrical shift of the HdS already reported for MENA. The distinctive behaviour of EA could be explained by the early HdS onset of this region already in the historical period (mid-May, the earliest of all MENA regions), as compared to the HdS retreat, which is comparable to that of the other regions (about mid-August).

The latitudinal differences reported for Start^{HdS} and End^{HdS} contribute to an even more pronounced latitudinal behaviour of the season lengthening, with a clear contrast between southern (0.93 day·year^{-1}) and northern (0.73 day·year^{-1}) latitudes, which means an HdS around 1 month longer in the former by the end of the century. Indeed, the largest and smallest trends in Length^{HdS} occur in WA (0.91 day·year^{-1}; approximately 120 days longer at the end of the century) and the IP (0.63 days·year^{-1}; or 80 days more with extreme conditions), respectively.

The projected changes in the HdS found here are in overall agreement with projections for the length of summer season reported elsewhere. For example, Park and Min (2018) evaluated the changes in the summer length for the Northern Hemisphere at 1.5 and 2.0° global warmings. Despite the lower radiative forcings employed therein, they found a generalized lengthening of the summer season, with larger advances in the summer onset

than delays in the summer retreat, as well as latitudinal differences involving more extended summers in mid- than in high-latitudes. Similar results have been reported for other regions, such as northern Europe (Ruosteenoja et al., 2020) or China (Deng et al., 2018). The change towards longer HdS in climate change scenarios is also in agreement with the longer summers reported in RCM-based projections for specific MENA sub-regions [e.g., Spain (De la Franca et al., 2013)]. By the end of the century, the summer lengthening for Spain was ~40 days, slightly lower than that obtained herein for the IP HdS (~60 days).

According to Figure 4, changes in the HdS already occur within the historical period, suggesting that they might also be detected in observations, assuming model realism and high signal-to-noise ratios in observations. The verification of these assumptions is particularly challenging for extremes, and in regions with low density, length and/or quality of observations, as Africa. Still, recent studies focusing on daily mean temperature observations have already identified changes towards a longer summer season in extratropical regions of the Northern Hemisphere (e.g., Park et al., 2018), Europe (Peña-Ortiz et al., 2015) or the Middle East (Goldreich and Chermoni, 2006), with overall larger changes in the summer onset than in the summer retreat. Some of the largest changes were reported in the Mediterranean region (partially covered by the MENA domain), where the summer has expanded towards earlier and later dates at different rates [23.6 days and 16.9 days, respectively, from 1953 to 2012; (Park et al., 2018)]. Some of the observed changes are comparable to those obtained for MENA over 1970–2010 (Figure 4), although this resemblance could be circumstantial, since estimates apply to different diagnostics (summer season vs. HdS) and regions, and observations and model simulations are affected by internal variability and model biases, respectively (e.g., Peña-Ortiz et al., 2015; Dosio, 2017).
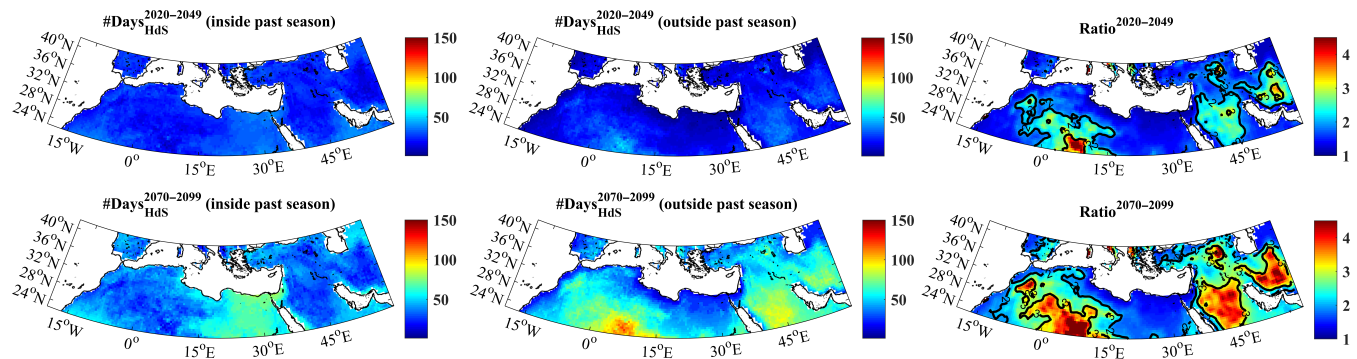
FIGURE 5 Number of hot days that are within (left column) and outside (middle column) the historical hot days season for the near and far futures under the RCP8.5 scenario. Frequency ratio (between the number of hot days that are outside and within the historical hot days season) for the near and far futures (right column) under the RCP8.5 scenario [Colour figure can be viewed at wileyonlinelibrary.com]

On the other hand, the latitudinal pattern of changes in the Length^{HdS} (Figure 3) resembles that found for the projected frequency of temperature extremes (Varela et al., 2020), which also shows a tendency for larger increases in the southernmost latitudes of MENA, as well as with recent observational trends in the frequency and duration of heat waves (Perkins-Kirkpatrick and Lewis, 2020). However, these changes do not inform on the frequency distribution of extremes with respect to the seasonal cycle. Therefore, we have evaluated here future changes in the timing of occurrence of hot days with respect to the historical HdS, which is relevant for impact assessments. These changes are expressed as the frequency ratio of future extremes occurring outside and inside the historical HdS. Values lower than 1 indicate that more than half of future extremes still occur during the historical season, while values higher than 1 imply more extremes shifted from the historical season, which poses additional threats for adaptation policies and early warning systems. Figure 5 represents the number of hot days that are within (left column) and outside (middle column) the historical HdS for the near and far future under the RCP8.5 scenario. Focusing on the near future (upper panels), the frequency of the days inside and outside the historical HdS is very similar (ratios of ~1), with the exception of a small area in southern-central Northern Africa dominated by shifted extremes. This picture changes for the far future (lower panels), when the HdS lengthening is so large that unusual timings dominate the frequency of extremes in MENA (ratios above 1). As expected, the fraction of extremes outside the historical HdS tends to be higher in areas where the increases in Length^{HdS} are also higher (Figure 3, right column). In the southern-central area of Northern Africa and PG, where the Length^{HdS} increases the most, dates outside the historical HdS largely account for extremes, with ratios well above two (up to 4.5). By the end of the century and RCP8.5, the only area

that keeps showing ratios around 1 (similar to those in the near future) is EA. This is also the southern region with the smallest changes in Length^{HdS}, and the longest HdS of MENA in the historical period (around 100 days), suggesting that climate change signals may have already emerged in that region by 1970–2005 leading to smaller future changes.

Thus, the projected lengthening of the HdS presented here would involve an earlier occurrence of hot days and could cause a corresponding shift in heat-related mortality (Muthers et al., 2010; Anderson and Bell, 2011; Founda et al., 2019). Moreover, Rohat et al. (2019), found that the number of people exposed to extreme heat in African cities will multiply by at least 20 by the end of the century. Exposure and vulnerability to extreme temperatures are more pronounced in many MENA countries than in other more developed areas (Niang et al., 2014; Russo et al., 2019a) due to the special characteristics of the MENA region as the higher levels of poverty, informal settlements and the need to work outdoors (Asefi-Najafabady et al., 2018; Watts et al., 2020). This fact delves in the importance to develop early warning systems that lessen the increasing risks of temperature extremes. Nevertheless, extreme temperatures are not systematically monitored in many countries of Africa (Harrington and Otto, 2020) hampering efforts to implement tailored adaptation and mitigation measures (Besada et al., 2009; Nyiwul, 2019). To deep further into local aspects, Table 2 shows the multi-model mean timing and length of the HdS (Start^{HdS}, End^{HdS} and Length^{HdS}) for the closest grid points to 15 MENA cities. The criterion for selecting these cities was: (a) cities with more than 1 million inhabitants (https://worldpopulationreview.com); and (b) one city per country that meets the above condition. The results are in overall agreement with the corresponding regional changes in HdS described above, although these local values should be considered for illustrative purposes only

TABLE 2 Multi-model mean of the seasonality of hot days (season start, end and length for the historical, near and far future periods) (mean ± 1 *SD*) for 15 specific CORDEX-MENA cities

	Historical: 1970–1999			Near future: 2020–2049			Far future: 2070–2099		
	Start^{HdS}	End^{HdS}	Length^{HdS}	Start^{HdS}	End^{HdS}	Length^{HdS}	Start^{HdS}	End^{HdS}	Length^{HdS}
Algiers	170 ± 14	257 ± 6	87 ± 15	153 ± 14	267 ± 6	114 ± 14	126 ± 18	284 ± 9	158 ± 19
Amman	163 ± 12	241 ± 7	78 ± 13	147 ± 12	255 ± 5	108 ± 15	116 ± 15	272 ± 8	156 ± 22
Baghdad	183 ± 8	230 ± 4	47 ± 10	166 ± 7	247 ± 4	81 ± 10	143 ± 12	264 ± 6	121 ± 18
Beirut	164 ± 19	252 ± 7	88 ± 18	146 ± 17	266 ± 9	120 ± 19	116 ± 17	283 ± 10	167 ± 24
Cairo	134 ± 17	234 ± 10	100 ± 14	118 ± 13	254 ± 7	136 ± 15	97 ± 10	271 ± 7	174 ± 15
Casablanca	164 ± 11	257 ± 6	93 ± 15	144 ± 16	268 ± 9	124 ± 23	114 ± 17	285 ± 11	171 ± 27
Damascus	173 ± 13	240 ± 7	67 ± 15	157 ± 15	255 ± 6	98 ± 19	129 ± 19	271 ± 9	142 ± 27
Dubai	170 ± 7	233 ± 4	63 ± 8	149 ± 6	252 ± 5	103 ± 10	123 ± 11	270 ± 6	147 ± 15
Istanbul	172 ± 18	245 ± 8	73 ± 17	159 ± 15	256 ± 9	97 ± 16	141 ± 16	272 ± 12	131 ± 23
Lisbon	176 ± 7	254 ± 5	78 ± 10	164 ± 9	263 ± 9	99 ± 15	144 ± 10	277 ± 7	133 ± 14
Madrid	183 ± 4	236 ± 4	53 ± 6	167 ± 5	248 ± 6	81 ± 9	150 ± 5	265 ± 6	115 ± 9
Riyadh	183 ± 8	228 ± 3	45 ± 9	158 ± 7	248 ± 3	90 ± 9	128 ± 9	268 ± 4	140 ± 12
Tehran	177 ± 4	228 ± 5	51 ± 6	163 ± 7	244 ± 4	81 ± 9	144 ± 11	262 ± 5	118 ± 15
Tripoli	140 ± 28	263 ± 6	123 ± 26	125 ± 22	275 ± 8	150 ± 21	98 ± 18	291 ± 9	193 ± 19
Tunis	170 ± 6	248 ± 5	78 ± 9	158 ± 9	257 ± 5	99 ± 12	134 ± 13	271 ± 6	137 ± 18

and taken with caution, as they are expected to be more affected by biases. These results are also in concordance with those obtained by Varela *et al.* (2020) who observed that more than 80% of the highly populated MENA cities will experience heat wave conditions during at least 50% of the warm season days by the end of the century. Our results emphasize the importance of seasonal shifts in the occurrence of extremes, many of which would occur outside of the historical season. This should be taken into account in the planning and implementation of strategies to cope with the projected increase of extremes in these vulnerable regions.

4 | CONCLUSIONS

An ensemble of RCM–GCM climate change CORDEX simulations over the Middle East–Northern Africa (MENA) region reveals a robust and pronounced lengthening of the season comprising hot days (HdS) during the 21st century. Changes in the length of the HdS (Length^{HdS}) arise from earlier onsets and delayed ends, but with an asymmetrical shift involving larger changes towards earlier dates. Under a RCP8.5 scenario, the multi-model mean onset of the HdS (Start^{HdS}) over MENA would advance almost 2 months at the end of the century, with extremely warm days typical of the summer season occurring by early May. A similar, albeit slightly

lower retreat is reported for the end of the HdS (End^{HdS}), which would extend to end September or early October by the end of the century. Together, these changes sum up to yield HdS about 3 months longer than in the historical period.

Late 21st changes in Length^{HdS} are not spatially uniform and range from 2 to 4 months across the MENA region, with the HdS lengthening increasing equatorwards, where the seasonal cycle and daily variability is less pronounced. This is in agreement with previous studies reporting dramatic increases in temperature extremes over tropical regions, where a permanent heat wave state could be approached (e.g., Perkins-Kirkpatrick and Gibson, 2017). In all MENA regions, the HdS advances more towards earlier dates than it retreats to later dates, with the exception of Eastern Africa.

The climate change projections towards longer HdS also involve pronounced changes in the timing of occurrence of hot days. By the end of the 21st century and RCP8.5, the number of extremes outside the historical HdS would on average outweigh by a factor of two those occurring within that season. The largest ratios are projected in the southern regions of MENA, with dramatic shifts (fourfold ratios) in Western Africa and the Persian Gulf. The exception is Eastern Africa, where the HdS lengthening is constrained by the comparatively earlier onset dates of the historical period. Taking into account these results and the particular conditions of the MENA

region, such as the continuous population increase or the lack of resources, the risks associated with extreme heat (such as migrations, mortality or famine) in the region are expected to increase dramatically.

The causes of the regional differences in the HdS (e.g., Eastern vs. Western Africa) require further research. Previous studies have reported that the underlying processes determining warm extremes in Northern Africa vary with the season (e.g., Fontaine et al., 2013) and the region (e.g., Guigma et al., 2020). The distinction of Eastern and Western Africa is supported by the main mode of inter-annual variability of hot days in observations, which displays a zonal dipole, indicating that hot days in Western Africa are not accompanied by extreme conditions in Eastern Africa, and vice versa (Guigma et al., 2020). In turn, this is in agreement with the spatial structure and propagation of the main synoptic patterns associated with heat waves (Moron et al., 2018), which include a diversity of phenomena, from travelling extratropical Rossby waves (mainly in the northern part of the region) to the Madden Julian Oscillation (with stronger effects towards the Sahel). Previous studies have mainly focused on heat waves over specific regions of Northern Africa, particularly the Sahel (to the south of the MENA region addressed here), with more emphasis on the western half of Northern Africa. For these regions, the main physical processes of extremely warm events have been related to warm advection and the greenhouse effect of water vapour (enhanced downward long wave radiation), sustained by southwesterly low-level moisture transport of water vapour from the Atlantic Ocean and/or the Western African Monsoon (e.g., Fontaine et al., 2013; Guigma et al., 2020). In particular, the water vapour effect plays a fundamental role during Sahelian heat waves and its long-term variations (Moron et al., 2018; Guigma et al., 2020), and could contribute to the enhanced meridional differences of the Length^{HdS} projections found herein (larger increases towards southern MENA under warmer/moister atmospheric conditions). However, water vapour content is also modulated by changes in its remote sources, transport and regional processes. For example, variations in the Western African Monsoon have been linked to sea surface temperature anomalies in the Atlantic and Indian oceans (e.g., Moron et al., 2018) as well as changes in the Saharan Heat Low through a water vapour–temperature feedback (Evan et al., 2015). It is not fully clear whether and how much the water vapour effect influences the HdS in the different MENA regions. Therefore, a more complete picture on the regional dynamics of hot days and their remote influences are required to gain understanding on the regional differences of the HdS reported here and their future changes.

ORCID

Rubén Varela [ID] https://orcid.org/0000-0001-9676-2349

REFERENCES

Ahmadalipour, A. and Moradkhani, H. (2018) Escalating heat-stress mortality risk due to global warming in the Middle East and North Africa (MENA). *Environment International*, 117, 215–225. https://doi.org/10.1016/j.envint.2018.05.014.

Ahmadalipour, A., Moradkhani, H. and Kumar, M. (2019) Mortality risk from heat stress expected to hit poorest nations the hardest. *Climatic Change*, 152(3–4), 569–579. https://doi.org/10.1007/s10584-018-2348-2.

Almazroui, M. (2019) Temperature changes over the CORDEX-MENA domain in the 21st century using CMIP5 data downscaled with RegCM4: A focus on the Arabian Peninsula. *Advances in Meteorology*, 2019, 1–18. https://doi.org/10.1155/2019/5395676.

Anderson, G.B. and Bell, M.L. (2011) Heat waves in the United States: mortality risk during heat waves and effect modification by heat wave characteristics in 43 US communities. *Environmental Health Perspectives*, 119(2), 210–218. https://doi.org/10.1289/ehp.1002313.

Argueso, D., Di Luca, A., Perkins-Kirkpatrick, S.E. and Evans, J.P. (2016) Seasonal mean temperature changes control future heat waves. *Geophysical Research Letters*, 43(14), 7653–7660. https://doi.org/10.1002/2016GL069408.

Asefi-Najafabady, S., Vandecar, K.L., Seimon, A., Lawrence, P. and Lawrence, D. (2018) Climate change, population, and poverty: vulnerability and exposure to heat stress in countries bordering the Great Lakes of Africa. *Climatic Change*, 148(4), 561–573. https://doi.org/10.1007/s10584-018-2211-5.

Barriopedro, D., Fischer, E.M., Luterbacher, J., Trigo, R.M. and García-Herrera, R. (2011) The hot summer of 2010: redrawing the temperature record map of Europe. *Science*, 332(6026), 220–224. https://doi.org/10.1126/science.1201224.

Besada, H., Lisk, F., Sewankambo, N., Kabasa, J. D., Sage, I., Willms, D., Werner, K., Orach, C. G., Isingoma, J. B. and Shaw, E. (2009). Climate change in Africa: Adaptation, mitigation and governance challenges.

Borghesi, S. and Ticci, E. (2019) Climate change in the MENA region: environmental risks, socioeconomic effects and policy challenges for the future. In: *IEMed: Mediterranean Yearbook*, Vol. 2019, pp. 289–292. Barcelona: European Institute of the Mediterranean.

Bucchignani, E., Mercogliano, P., Panitz, H.J. and Montesarchio, M. (2018) Climate change projections for the Middle East–North Africa domain with COSMO-CLM at different spatial resolutions. *Advances in Climate Change Research*, 9(1), 66–80. https://doi.org/10.1016/j.accre.2018.01.004.

Cassou, C. and Cattiaux, J. (2016) Disruption of the European climate seasonal clock in a warming world. *Nature Climate Change*, 6, 589–594. https://doi.org/10.1038/nclimate2969.

Christensen, O.B., Gutowski, W.J., Nikulin, G. and Legutke, S. (2014) *CORDEX Archive design*. Copenhague: Danish Meteorological Institute.

Christidis, N., Stott, P.A., Brown, S., Karoly, D.J. and Caesar, J. (2007) Human contribution to the lengthening of the growing season during 1950–99. *Journal of Climate*, 20, 5441–5454. https://doi.org/10.1175/2007JCLI1568.1.

Cramer, W., Guiot, J., Fader, M., Garrabou, J., Gattuso, J.P., Iglesias, A., Lange, M.A., Lionello, P., Llasat, M.C., Paz, S., Penuelas, J., Snoussi, M., Toreti, A., Tsimplis, M.N. and Xoplaki, E. (2018) Climate change and interconnected risks to sustainable development in the Mediterranean. *Nature Climate Change*, 8(11), 972–980. https://doi.org/10.1038/s41558-018-0299-2.

de Castro, M., Gómez-Gesteira, M., Ramos, A.M., Álvarez, I. and de Castro, P. (2011) Effects of heat waves on human mortality, Galicia, Spain. *Climate Research*, 48, 333–341. https://doi.org/10.3354/cr00988.

de la Franca, N.L., Sánchez, E. and Domínguez, M. (2013) Changes in the onset and length of seasons from an ensemble of regional climate models over Spain for future climate conditions. *Theoretical and Applied Climatology*, 114(3–4), 635–642. https://doi.org/10.1007/s00704-013-0868-2.

Deng, H., Yin, Y. and Wu, S. (2018) Divergent responses of thermal growing degree-days and season to projected warming over China. *International Journal of Climatology*, 38, 5605–5618. https://doi.org/10.1002/joc.5766.

Dosio, A. (2017) Projection of temperature and heat waves for Africa with an ensemble of CORDEX Regional Climate Models. *Climate Dynamics*, 49(1–2), 493–519. https://doi.org/10.1007/s00382-016-3355-5.

Dosio, A. and Panitz, H.J. (2016) Climate change projections for CORDEX-Africa with COSMO-CLM regional climate model and differences with the driving global climate models. *Climate Dynamics*, 46(5–6), 1599–1625. https://doi.org/10.1007/s00382-015-2664-4.

Driouech, F., ElRhaz, K., Moufouma-Okia, W., Arjdal, K. and Balhane, S. (2020) Assessing future changes of climate extreme events in the CORDEX-MENA region using regional climate model ALADIN-climate. *Earth Systems and Environment*, 4(3), 477–492. https://doi.org/10.1007/s41748-020-00169-3.

Easterling, D.R. (2002) Recent changes in frost days and the frost-free season in the United States. *Bulletin of the American Meteorological Society*, 83(9), 1327–1332. https://doi.org/10.1175/1520-0477-83.9.1327.

Evan, A.T., Flamant, C., Lavaysse, C., Kocha, C. and Saci, A. (2015) Water vapor–forced greenhouse warming over the Sahara Desert and the recent recovery from the Sahelian drought. *Journal of Climate*, 28(1), 108–123. https://doi.org/10.1175/JCLI-D-14-00039.1.

Evans, J.P. (2009) 21st century climate change in the Middle East. *Climatic Change*, 92(3–4), 417–432. https://doi.org/10.1007/s10584-008-9438-5.

Fontaine, B., Janicot, S. and Monerie, P.A. (2013) Recent changes in air temperature, heat waves occurrences, and atmospheric circulation in Northern Africa. *Journal of Geophysical Research, [Atmospheres]*, 118(15), 8536–8552. https://doi.org/10.1002/jgrd.50667.

Founda, D., Varotsos, K.V., Pierros, F. and Giannakopoulos, C. (2019) Observed and projected shifts in hot extremes' season in the Eastern Mediterranean. *Global and Planetary Change*, 175, 190–200. https://doi.org/10.1016/j.gloplacha.2019.02.012.

García-Herrera, R., Díaz, J., Trigo, R.M., Luterbacher, J. and Fischer, E. M. (2010) A review of the European summer heat wave of 2003. *Critical Reviews in Environmental Science and Technology*, 40(4), 267–306. https://doi.org/10.1080/10643380802238137.

Gasparrini, A., Guo, Y., Sera, F., Vicedo-Cabrera, A.M., Huber, V., Tong, S., de Sousa Zanotti Stagliorio Coelho, M., Nascimento Saldiva, P.H., Lavigne, E., Matus Correa, P., Valdes Ortega, N., Kan, H., Osorio, S., Kyselý, J., Urban, A., Jaakkola, J.J.K., Ryti, N.R.I., Pascal, M., Goodman, P.G., Zeka, A., Michelozzi, P., Scortichini, M., Hashizume, M., Honda, Y., Hurtado-Diaz, M., Cesar Cruz, J., Seposo, X., Kim, H., Tobias, A., Iñiguez, C., Forsberg, B., Åström, D.O., Ragettli, M.S., Guo, Y.L., Wu, C.F., Zanobetti, A., Schwartz, J., Bell, M.L., Dang, T.N., Van, D.D., Heaviside, C., Vardoulakis, S., Hajat, S., Haines, A. and Armstrong, B. (2017) Projections of temperature-related excess mortality under climate change scenarios. *Lancet Planet Health*, 1(9), e360–e367. https://doi.org/10.1016/S2542-5196(17)30156-0.

Giorgi, F. and Lionello, P. (2008) Climate change projections for the Mediterranean region. *Global and Planetary Change*, 63(2–3), 90–104. https://doi.org/10.1016/j.gloplacha.2007.09.005.

Giugni, M., Simonis, I., Bucchignani, E., Capuano, P., De Paola, F., Engelbrecht, F., Mercogliano, P. and Topa, M.E. (2015) The impacts of climate change on African cities. In: *Urban Vulnerability and Climate Change in Africa*. Cham: Springer, pp. 37–75. https://doi.org/10.1007/978-3-319-03982-4_2.

Goldreich, Y. and Chermoni, Z. (2006). The changes in the summer season length in the Middle East. *International Conference on Climate Change and the Middle East: Past, Present and Future*.

Göll, E. (2017). Future challenges of climate change in the MENA region. CIDOB.

Grant, A., Burger, N. and Wodon, Q. (2014). Climate-induced migration in the MENA region: results from the qualitative fieldwork.

Guigma, K.H., Todd, M. and Wang, Y. (2020) Characteristics and thermodynamics of Sahelian heatwaves analysed using various thermal indices. *Climate Dynamics*, 55(11), 3151–3175. https://doi.org/10.1007/s00382-020-05438-5.

Hameed, M., Moradkhani, H., Ahmadalipour, A., Moftakhari, H., Abbaszadeh, P. and Alipour, A. (2019) A review of the 21st century challenges in the food-energy-water security in the Middle East. *Water*, 11(4), 682. https://doi.org/10.3390/w11040682.

Harrington, L.J. and Otto, F.E. (2020) Reconciling theory with the reality of African heatwaves. *Nature Climate Change*, 10(9), 796–798. https://doi.org/10.1038/s41558-020-0851-8.

Hersbach, H., Bell, B., Berrisford, P., Hirahara, S., Horányi, A., Muñoz-Sabater, J., Nicolas, J., Peubey, C., Radu, R., Schepers, D., Simmons, A., Soci, C., Abdalla, S., Abellan, X., Balsamo, G., Bechtold, P., Biavati, G., Bidlot, J., Bonavita, M., Chiara, G., Dahlgren, P., Dee, D., Diamantakis, M., Dragani, R., Flemming, J., Forbes, R., Fuentes, M., Geer, A., Haimberger, L., Healy, S., Hogan, R.J., Hólm, E., Janisková, M., Keeley, S., Laloyaux, P., Lopez, P., Lupu, C., Radnoti, G., Rosnay, P., Rozum, I., Vamborg, F., Villaume, S. and Thépaut, J.N. (2020) The ERA5 global reanalysis. *Quarterly Journal of the Royal Meteorological Society*, 146, 1999–2049. https://doi.org/10.1002/qj.3803.

Jacob, D., Petersen, J., Eggert, B., Alias, A., Christensen, O.B., Bouwer, L.M., Braun, A., Colette, A., Déqué, M.,

Georgievski, G., Georgopoulou, E., Gobiet, A., Menut, L., Nikulin, G., Haensler, A., Hempelmann, N., Jones, C., Keuler, K., Kovats, S., Kröner, N., Kotlarski, S., Kriegsmann, A., Martin, E., van Meijgaard, E., Moseley, C., Pfeifer, S., Preuschmann, S., Radermacher, C., Radtke, K., Rechid, D., Rounsevell, M., Samuelsson, P., Somot, S., Soussana, J.F., Teichmann, C., Valentini, R., Vautard, R., Weber, B. and Yiou, P. (2014) EURO-CORDEX: new high-resolution climate change projections for European impact research. *Regional Environmental Change*, 14(2), 563–578. https://doi.org/10.1007/s10113-013-0499-2.

Kjellstrom, T., Freyberg, C., Lemke, B., Otto, M. and Briggs, D. (2018) Estimating population heat exposure and impacts on working people in conjunction with climate change. *International Journal of Biometeorology*, 62(3), 291–306. https://doi.org/10.1007/s00484-017-1407-0.

Kornhuber, K., Coumou, D., Vogel, E., Lesk, C., Donges, J.F., Lehmann, J. and Horton, R.M. (2020) Amplified Rossby waves enhance risk of concurrent heatwaves in major breadbasket regions. *Nature Climate Change*, 10(1), 48–53. https://doi.org/10.1038/s41558-019-0637-z.

Kunkel, K.E., Easterling, D.R., Hubbard, K. and Redmond, K. (2004) Temporal variations in frost-free season in the United States: 1895–2000. *Geophysical Research Letters*, 31(3), L03201. https://doi.org/10.1029/2003GL018624.

Lange, M.A. (2019) Impacts of climate change on the Eastern Mediterranean and the Middle East and North Africa region and the water–energy nexus. *Atmosphere*, 10(8), 455. https://doi.org/10.3390/atmos10080455.

Lelieveld, J., Proestos, Y., Hadjinicolaou, P., Tanarhte, M., Tyrlis, E. and Zittis, G. (2016) Strongly increasing heat extremes in the Middle East and North Africa (MENA) in the 21st century. *Climatic Change*, 137(1–2), 245–260. https://doi.org/10.1007/s10584-016-1665-6.

Miralles, D.G., Gentine, P., Seneviratne, S.I. and Teuling, A.J. (2019) Land–atmospheric feedbacks during droughts and heatwaves: state of the science and current challenges. *Annals of the New York Academy of Sciences*, 1436(1), 19–35. https://doi.org/10.1111/nyas.13912.

Mora, C., Dousset, B., Caldwell, I.R., Powell, F.E., Geronimo, R.C., Bielecki, C.R., Counsell, C.W.W., Dietrich, B.S., Johnston, E.T., Louis, L.V., Lucas, M.P., McKenzie, M.M., Shea, A.G., Tseng, H., Giambelluca, T.W., Leon, L.R., Hawkins, E. and Trauernicht, C. (2017) Global risk of deadly heat. *Nature Climate Change*, 7(7), 501–506. https://doi.org/10.1038/nclimate3322.

Moron, V., Oueslati, B., Pohl, B. and Janicot, S. (2018) Daily weather types in February–June (1979–2016) and temperature variations in tropical North Africa. *Journal of Applied Meteorology and Climatology*, 57(5), 1171–1195. https://doi.org/10.1175/JAMC-D-17-0105.1.

Murray, V. and Ebi, K.L. (2012) IPCC special report on managing the risks of extreme events and disasters to advance climate change adaptation (SREX). *BMJ Journals*, 66, 759–760. https://doi.org/10.1136/jech-2012-201045.

Muthers, S., Matzarakis, A. and Koch, E. (2010) Summer climate and mortality in Vienna–a human-biometeorological approach of heat-related mortality during the heat waves in 2003. *Wiener Klinische Wochenschrift*, 122(17–18), 525–531. https://doi.org/10.1007/s00508-010-1424-z.

Ncube, M., Anyanwu, J.C. and Hausken, K. (2014) Inequality, economic growth and poverty in the Middle East and North Africa (MENA). *African Development Review*, 26(3), 435–453. https://doi.org/10.1111/1467-8268.12103.

Niang, I., Ruppel, O.C., Abdrabo, M.A., Essel, A., Lennard, C., Padgham, J. and Urquhart, P. (2014) Africa. In: Barros, V.R., Field, C.B., Dokken, D.J., Mastrandrea, M.D., Mach, K.J., Bilir, T.E., Chatterjee, M., Ebi, K.L., Estrada, Y.O., Genova, R. C., Girma, B., Kissel, E.S., Levy, A.N., MacCracken, S., Mastrandrea, P.R. and White, L.L. (Eds.) *Climate Change 2014: Impacts, Adaptation, and Vulnerability. Part B: Regional Aspects. Contribution of Working Group II to the Fifth Assessment Report of the Intergovernmental Panel on Climate Change.* Cambridge, United Kingdom and New York, NY: Cambridge University Press, pp. 1199–1265.

Ntoumos, A., Hadjinicolaou, P., Zittis, G. and Lelieveld, J. (2020) Updated assessment of temperature extremes over the Middle East–North Africa (MENA) region from observational and CMIP5 data. *Atmosphere*, 11(8), 813. https://doi.org/10.3390/atmos11080813.

Nyiwul, L.M. (2019) Climate change mitigation and adaptation in africa: strategies, synergies, and constraints. In: *Climate Change and Global Development*. Cham: Springer, pp. 219–241. https://doi.org/10.1007/978-3-030-02662-2_11.

Ozturk, T., Turp, M.T., Türkeş, M. and Kurnaz, M.L. (2018) Future projections of temperature and precipitation climatology for CORDEX-MENA domain using RegCM4.4. *Atmospheric Research*, 206, 87–107. https://doi.org/10.1016/j.atmosres.2018.02.009.

Pal, J.S. and Eltahir, E.A. (2016) Future temperature in southwest Asia projected to exceed a threshold for human adaptability. *Nature Climate Change*, 6(2), 197–200. https://doi.org/10.1038/nclimate2833.

Park, B.J., Kim, Y.H., Min, S.K. and Lim, E.P. (2018) Anthropogenic and natural contributions to the lengthening of the summer season in the Northern Hemisphere. *Journal of Climate*, 31(17), 6803–6819. https://doi.org/10.1175/JCLI-D-17-0643.1.

Park, B. J., and Min, S. K. (2018). Northern Hemisphere summer season lengthening at 1.5 and 2.0 degree global warming. EGUGA, 5785.

Peña-Ortiz, C., Barriopedro, D. and García-Herrera, R. (2015) Multidecadal variability of the summer length in Europe. *Journal of Climate*, 28(13), 5375–5388. https://doi.org/10.1175/JCLI-D-14-00429.1.

Perkins-Kirkpatrick, S.E. and Gibson, P.B. (2017) Changes in regional heatwave characteristics as a function of increasing global temperature. *Scientific Reports*, 7(1), 1–12. https://doi.org/10.1038/s41598-017-12520-2.

Perkins-Kirkpatrick, S.E. and Lewis, S.C. (2020) Increasing trends in regional heatwaves. *Nature Communications*, 11(1), 1–8. https://doi.org/10.1038/s41467-020-16970-7.

Pierce, D.W., Barnett, T.P., Santer, B.D. and Gleckler, P.J. (2009) Selecting global climate models for regional climate change studies. *Proceedings of the National Academy of Sciences*, 106(21), 8441–8446. https://doi.org/10.1073/pnas.0900094106.

Rohat, G., Flacke, J., Dosio, A., Dao, H. and van Maarseveen, M. (2019) Projections of human exposure to dangerous heat in African cities under multiple socioeconomic and climate scenarios. *Earth's Future*, 7(5), 528–546. https://doi.org/10.1029/2018EF001020.

Ruosteenoja, K., Markkanen, T. and Räisänen, J. (2020) Thermal seasons in northern Europe in projected future climate.

International Journal of Climatology, 40, 4444–4462. https://doi.org/10.1002/joc.6466.

Russo, A., Gouveia, C.M., Dutra, E., Soares, P.M.M. and Trigo, R.M. (2019b) The synergy between drought and extremely hot summers in the Mediterranean. *Environmental Research Letters*, 14(1), 014011. https://doi.org/10.1088/1748-9326/aaf09e.

Russo, S., Marchese, A.F., Sillmann, J. and Imme, G. (2016) When will unusual heat waves become normal in a warming Africa? *Environmental Research Letters*, 11(5), 054016. https://doi.org/10.1088/1748-9326/11/5/054016.

Russo, S., Sillmann, J., Sippel, S., Barcikowska, M.J., Ghisetti, C., Smid, M. and O'Neill, B. (2019a) Half a degree and rapid socioeconomic development matter for heatwave risk. *Nature Communications*, 10(1), 1–9. https://doi.org/10.1038/s41467-018-08070-4.

Sánchez-Benítez, A., García-Herrera, R., Barriopedro, D., Sousa, P.M. and Trigo, R.M. (2018) June 2017: the earliest European summer mega-heatwave of Reanalysis Period. *Geophysical Research Letters*, 45(4), 1955–1962. https://doi.org/10.1002/2018GL077253.

Sheridan, S.C. and Lin, S. (2014) Assessing variability in the impacts of heat on health outcomes in New York City over time, season, and heat-wave duration. *EcoHealth*, 11(4), 512–525. https://doi.org/10.1007/s10393-014-0970-7.

Smith, K.R., Woodward, A., Campbell-Lendrum, D., et al. (2014) Human health: impacts, adaptation, and co-benefits. In: Field, C.B., Barros, V.R., Dokken, D.J., et al. (Eds.) *Climate Change: Impacts, Adaptation, and Vulnerability. Part A: Global and Sectoral Aspects. Contribution of Working Group II to the fifth assessment report of the Intergovernmental Panel on Climate Change*, Vol. 2014. Cambridge: Cambridge University Press, pp. 709–754.

Stine, A., Huybers, P. and Fung, I. (2009) Changes in the phase of the annual cycle of surface temperature. *Nature*, 457(7228), 435–440. https://doi.org/10.1038/nature07675.

Taylor, K.E., Stouffer, R.J. and Meehl, G.A. (2012) An overview of CMIP5 and the experiment design. *Bulletin of the American Meteorological Society*, 93, 485–498. https://doi.org/10.1175/BAMS-D-11-00094.1.

Varela, R., Rodríguez-Díaz, L. and de Castro, M. (2020) Persistent heat waves projected for Middle East and North Africa by the end of the 21st century. *PLoS One*, 15(11), e0242477. https://doi.org/10.1371/journal.pone.0242477.

Waha, K., Krummenauer, L., Adams, S., Aich, V., Baarsch, F., Coumou, D., Fader, M., Hoff, H., Jobbins, G., Marcus, R., Mengel, M., Otto, I.M., Perrette, M., Rocha, M., Robinson, A. and Schleussner, C.-F. (2017) Climate change impacts in the Middle East and Northern Africa (MENA) region and their implications for vulnerable population groups. *Regional Environmental Change*, 17(6), 1623–1638. https://doi.org/10.1007/s10113-017-1144-2.

Watts, N., Adger, W.N., Agnolucci, P., Blackstock, J., Byass, P., Cai, W., Chaytor, S., Colbourn, T., Collins, M., Cooper, A., Cox, P.M., Depledge, J., Drummond, P., Ekins, P., Galaz, V., Grace, D., Graham, H., Grubb, M., Haines, A., Hamilton, I., Hunter, A., Jiang, X., Li, M., Kelman, I., Liang, L., Lott, M., Lowe, R., Luo, Y., Mace, G., Maslin, M., Nilsson, M., Oreszczyn, T., Pye, S., Quinn, T., Svensdotter, M., Venevsky, S., Warner, K., Xu, B., Yang, J., Yin, Y., Yu, C., Zhang, Q., Gong, P., Montgomery, H. and Costello, A. (2015) Health and climate change: policy responses to protect public health. *Lancet*, 386, 1861–1914. https://doi.org/10.1016/S0140-6736(15)60854-6.

Watts, N., Amann, M., Arnell, N., Ayeb-Karlsson, S., Beagley, J., Belesova, K., Boykoff, M., Byass, P., Cai, W., Campbell-Lendrum, D., Capstick, S., Chambers, J., Coleman, S., Dalin, C., Daly, M., Dasandi, N., Dasgupta, S., Davies, M., di Napoli, C., Dominguez-Salas, P., Drummond, P., Dubrow, R., Ebi, K.L., Eckelman, M., Ekins, P., Escobar, L.E., Georgeson, L., Golder, S., Grace, D., Graham, H., Haggar, P., Hamilton, I., Hartinger, S., Hess, J., Hsu, S.C., Hughes, N., Jankin Mikhaylov, S., Jimenez, M.P., Kelman, I., Kennard, H., Kiesewetter, G., Kinney, P.L., Kjellstrom, T., Kniveton, D., Lampard, P., Lemke, B., Liu, Y., Liu, Z., Lott, M., Lowe, R., Martinez-Urtaza, J., Maslin, M., McAllister, L., McGushin, A., McMichael, C., Milner, J., Moradi-Lakeh, M., Morrissey, K., Munzert, S., Murray, K.A., Neville, T., Nilsson, M., Sewe, M.O., Oreszczyn, T., Otto, M., Owfi, F., Pearman, O., Pencheon, D., Quinn, R., Rabbaniha, M., Robinson, E., Rocklöv, J., Romanello, M., Semenza, J.C., Sherman, J., Shi, L., Springmann, M., Tabatabaei, M., Taylor, J., Triñanes, J., Shumake-Guillemot, J., Vu, B., Wilkinson, P., Winning, M., Gong, P., Montgomery, H. and Costello, A. (2020) The 2020 report of The Lancet Countdown on health and climate change: responding to converging crises. *The Lancet.*, 397, 129–170. https://doi.org/10.1016/S0140-6736(20)32290-X.

Watts, N., Amann, M., Arnell, N., Ayeb-Karlsson, S., Belesova, K., Boykoff, M., Byass, P., Cai, W., Campbell-Lendrum, D., Capstick, S., Chambers, J., Dalin, C., Daly, M., Dasandi, N., Davies, M., Drummond, P., Dubrow, R., Ebi, K.L., Eckelman, M., Ekins, P., Escobar, L.E., Fernandez Montoya, L., Georgeson, L., Graham, H., Haggar, P., Hamilton, I., Hartinger, S., Hess, J., Kelman, I., Kiesewetter, G., Kjellstrom, T., Kniveton, D., Lemke, B., Liu, Y., Lott, M., Lowe, R., Sewe, M.O., Martinez-Urtaza, J., Maslin, M., McAllister, L., McGushin, A., Jankin Mikhaylov, S., Milner, J., Moradi-Lakeh, M., Morrissey, K., Murray, K., Munzert, S., Nilsson, M., Neville, T., Oreszczyn, T., Owfi, F., Pearman, O., Pencheon, D., Phung, D., Pye, S., Quinn, R., Rabbaniha, M., Robinson, E., Rocklöv, J., Semenza, J.C., Sherman, J., Shumake-Guillemot, J., Tabatabaei, M., Taylor, J., Trinanes, J., Wilkinson, P., Costello, A., Gong, P. and Montgomery, H. (2019) The 2019 report of The Lancet Countdown on health and climate change: ensuring that the health of a child born today is not defined by a changing climate. *The Lancet*, 394(10211), 1836–1878. https://doi.org/10.1016/S0140-6736(19)32596-6.

Wodon, Q., Burger, N., Grant, A. and Liverani, A. (2014). Climate change, migration, and adaptation in the MENA Region.

SUPPORTING INFORMATION

Additional supporting information may be found in the online version of the article at the publisher's website.

How to cite this article: Varela, R., Rodríguez-Díaz, L., Barriopedro, D., de Castro, M., Costoya, X., García-Herrera, R., & Gómez-Gesteira, M. (2022). Projected changes in the season of hot days in the Middle East and North Africa. *International Journal of Climatology*, 42(4), 2195–2207. https://doi.org/10.1002/joc.7360